Polymer Journal, Vol. 15, No. 3, pp 179—193 (1983)

Surface Diffusion Flow on the Pore Wall When Gas Permeates through a Polymeric Membrane

Kenji KAMIDE, Sei-ichi MANABE, Hiroyuki MAKINO, Takashi NOHMI, Hiroki NARITA, and Toru KAWAI*

Textile Research Laboratory, Asahi Chemical Industry Ltd., Takatsuki, Osaka 567, Japan
**Department of Clothings, Tanaka Chiyo Women's College, Machida, Tokyo 194, Japan*

(Received August 18, 1982)

ABSTRACT: In order to explain the difference between measured and calculated gas permeability coefficinets $\boldsymbol{P}(P_1, P_1)$ for a polymeric membrane dominated by free molecular flow, the surface diffusion flow was taken into account. The equation for $\boldsymbol{P}(P_1, P_1)$ in the case where these two flows occur concurrently was derived on the basis of the following assumptions: (1) The transport of a gas through a fine tube is given by

$$\dot{n} = -2\pi r D_s \frac{d\sigma}{dx} - \frac{8}{3}\frac{2-f_0}{f_0}\frac{[r-a(p)]^3}{(2\pi mkT)^{1/2}}\frac{dP}{dx}$$

where $\dot{n}$ is the net flux of molecules at the position x, σ, the surface concentration of sorbed molecules on the tube wall, r, the radius of the tube, f_0, Maxwell's reflection coefficient associated with the free molecular flow, m, the mass of one gas molecule, $a(p)$, the thickness of the absorved gas layer, and P and T, the pressure and temperature of the gas, respectively. (2) σ is represented by the BET equation as a function of P and T. The expression of $\boldsymbol{P}(P_1, P_1)$ for a porous membrane having a wide pore size distribution was derived by solving the above equation when the total gas flux is the sum of the fluxes through the individual pores. The calculated values of $\boldsymbol{P}(P_1, P_1)$ for a polycarbonate membrane having straight-through pores agreed with the experimental values.

KEY WORDS Gas Permeation / Porous Polymeric Membrane / Surface Diffusion Flow / Free Molecular Flow / Straight-Through Pore / Pore Size Distribution / Polycarbonate Membrane / Cellulose Acetate Membrane /

The permeation mechanism of an inorganic gas through a straight-through porous polymeric membrane, whose pore radius $\bar{r}_3$ (the third mean radius defined later) is larger than 18 nm, was recently proposed by us.[1-4] When $\bar{r}_3$ is larger than 18 nm, the following three flows occur: a viscous flow including a slip flow (referred to as the V flow), a free molecular flow (the F flow), and V and F flows combined in series (the VF flow[1]).

Reported gas permeation data of organic gases for polymeric membranes are too few to clarify the permeation mchanism involved. In our previous study,[3] an unusually high permeability coefficient was found for organic gases in a polycarbonate membrane with an $\bar{r}_3$ of 18 nm. The difference between the experimental permeability coefficient $\boldsymbol{P}(P_1,P_1)$ and the theoretical F flow permeability coefficient was represented as a function of the boiling points of the organic gases employed. We were of the opinion[3] that the observed unusually rapid gas permeation might be due mainly to the surface diffusion flow (S flow). No detailed quantitative evaluation of this flow was made in previous papers[3,4] in which the permeability coefficient for the S flow was assumed with no theoretical basis. In this report, the theoretical equation for this permeability coefficient is derived and applied to the present and previous experimental data.

THEORETICAL

Derivation of the Permeability Coefficient of the

Surface Diffusion Flow in a Cylindrical Pore by Using Hill's Theory[6]

The flow of gas through fine pores of a membrane is determined primarily by free molecular flow when the pressure difference across the membrane is low and the pore size is sufficiently small compared to the mean free path of gas molecules.[3] Under these conditions, the steady-state flux of gas molecules, $\dot{n}$, passing over the cross section at a position x from the inlet of the tube is given by Sear[5] as follows:

$$\dot{n} = -D_s\theta\frac{d\sigma}{dx} - \frac{8}{3}\left(\frac{2}{\pi mkT}\right)^{1/2}\frac{A^2}{\theta}\frac{dP}{dx} \tag{1}$$

where σ is the surface concentration of adsorbed molecules on the pore wall, A, the cross-sectional area of the tube, θ, the cross-sectional periphery, m, the mass of one molecules, and D_s, the surface diffusion coefficient.

On integrating eq 1 when $P=P_1$ at $x=0$ and $P=P_2$ at $x=d$ (d, tube length), Hill[6] derived the following equations for the case where the adsorbed phase is a perfect two-dimensional gas and thermodynamic equilibrium is always established in the absorption/desorption process:

$$-\dot{n}x = \frac{\theta}{4D_0}\left(\frac{\pi kT}{2m}\right)^{1/2}\ln\frac{P}{P_1} + \frac{16}{3}\frac{A^2}{\theta(2\pi mkT)^{1/2}}(P-P_1) \tag{2}$$

$$\frac{x}{d}\left[K\ln\frac{P_2}{P_1} + \left(\frac{P_2}{P_1}-1\right)\right] = K\ln\frac{P}{P_1} + \left(\frac{P}{P_1}-1\right) \tag{3}$$

with

$$K = \frac{3\pi kT}{16a_t^2 D_0 P} \tag{4}$$

where a_t is the radius of the tube and D_0 is the diameter of the sorbed molecule.

Figure 1 shows a schematic representation of gas permeation through a pore. In this figure, r is the pore radius, d the membrane thickness, and $a(p)$, the thickness of the layer of sorbed molecules on the pore wall at pressure P. The pressure P decreases from P_1 at the inlet of the pore to P_2 at the outlet. x is the distance from the membrane surface in the direction of membrane thickness.

Since the pore size is assumed to be too small to allow a viscous flow to occur, eq 1 holds for gas permeation through a cylindrical pore. Hence, the fundamental isothermal steady-state transport equation for gas molecules is given by

$$\dot{n} = -2\pi rD_s\frac{d\sigma}{dx} - \frac{8}{3}\frac{2-f_0}{f_0}\frac{\pi^2r^4}{\pi r(2\pi mkT)^{1/2}}\frac{dP}{dx} \tag{5}$$

where f_0 is Maxwell's reflection coefficient associated with the free molecular flow and is neglected in Sear's equation (eq 1). The first term on the right-hand side of eq 5 represents the surface diffusion flow and the second term the free molecular flow (F flow).

If the absorbed layer is a perfect two-dimensional gas, then D_s is obtained as a function of P using the kinetic theory of a two dimensional gas. Integration of eq 5 from $x=0$ to $x=d$ with σ dependent linearly on P gives

$$-\dot{n}d = \frac{2\pi r}{4D_0}\left(\frac{\pi kT}{2m}\right)^{1/2}\ln\frac{P_2}{P_1} + \frac{8}{3}\frac{2-f_0}{f_0}\frac{\pi r^3}{(2\pi mkT)^{1/2}}(P_2-P_1) \tag{6}$$

The gas permeation coefficient $\boldsymbol{P}_c(P_1, P_2)'$ for a cylindrical pore is defined as

$$\boldsymbol{P}_c(P_1, P_2)' = -\frac{d}{N_A}\dot{n}\left(\frac{1}{P_2-P_1}\right) \tag{7}$$

where N_A is Avogadro's constant. The prime indicates the gas permeation coefficient expressed in units of mol/cm·cmHg·s.

Substitution of eq 6 into eq 7 lead to

$$\boldsymbol{P}_c(P_1, P_2)' = \boldsymbol{P}_s' + \boldsymbol{P}_f' \tag{8}$$

with

$$\boldsymbol{P}_s' = r(\pi RT)^{3/2}(\ln P_1/P_2)/\times[z(P_1-P_2)2D_0N_A(2M)^{1/2}RT] \tag{9}$$

$$\boldsymbol{P}_f' = [(2-f_0)/f_0](4r^3/3)(2\pi RT/M)^{1/2}/RT \tag{10}$$

where z is the conversion factor of pressure from cmHg to dyn/cm^2, and equals $1.01325\times10^6/76.0$. Equations 9 and 10 were presented in our previous paper[1] without any detailed derivations.

Theoretically Rigorous Equation for the Permeability Coefficient of Surface Diffusion Flow in a Cylindrical Pore

As shown in Figure 1, the pore size effective for free molecular flow varies with the thickness of the absorbed gas layer $a(p)$, which may be approximated by the product of the molecular diameter and the number of molecules in the absorbed gas layer

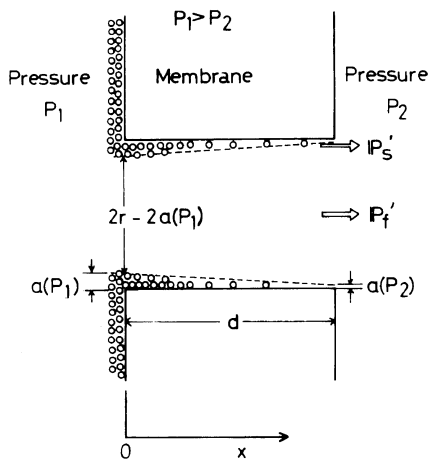

Figure 1. Schematic representation of gas permeation through a membrane pore: open circles, absorbed gas molecules; broken lines, thickness of the layer of absorbed molecules; $\boldsymbol{P}_s'$, permeability coefficient for the flow of absorbed molecules, *i.e.*, surface diffusion flow; $\boldsymbol{P}_f'$, permeability coefficient for the flow of free molecules, *i.e.*, free molecular flow; 0 indicates the position of the upstream membrane surface.

[*i.e.*, $D_0\sigma/(N_A \cdot v_{as})$; v_{as}, the moles necessary to build up a unit area of a mono-absorbed layer].

The fundamental transport equation corresponding to eq 5 is

$$\dot{n} = -2\pi r D_s(\mathrm{d}\sigma/\mathrm{d}x) - (8/3)[(2-f_0)/f_0] \times [r-a(p)]^3[\pi/(2\pi mkT)^{1/2}](\mathrm{d}P/\mathrm{d}x) \quad (11)$$

Here, $[r-a(p)]$ can be approximated by $\{r-[a(p_1)+a(p_2)]/2\}$ for P between P_1 and P_2, because $r \gg a(p)$. When $a(p)$ equals zero, eq 11 reduces to eq 5.

The absorbed gas is assumed to form a multilayer. Then, the surface concentration of absorbed gas molecules may be given by the BET equation[7]:

$$\sigma/N_A = v_{as}\gamma x'/[(1-x')(1-x'+\gamma x')] \quad (12)$$

where v_{as} is the moles neccessary to build a complete mono-absorbed layer, x', the saturated vapor pressure P_0 relative to the pressure P of the permeating gas, *i.e.*, $x' = P/P_0$, and γ is a constant related to the interaction between the permeating gas and the membrane material, represented by

$$\gamma = \exp(E_1 - E_2)/RT \quad (13)$$

where E_1 is the heat of absorption and E_2 is the heat of condensation of the gas.

A reasonable first approximation is that the gas molecules absorbed on the pore wall behave as a two-dimensinal ideal gas and that the gas molecules in the vicinity of the absorbed layer and the pore wall behave as a three-dimensional ideal gas. Thus, the mean velocity, m_v, of molecules absorbed on the pore wall may be expressed by[7] $m_v = [\pi mkT/(2m)]^{1/2}$. The mean free path of absorbed molecules, $\lambda_{2,a}$, is not equal to the mean free path in a free two-dimensional gas, $\lambda_{2,i}$, but must be corrected for the existence of neighboring gas molecules. With an increase in σ, $\lambda_{2,a}$ may approach $\lambda_{2,i}$, while as σ decrease to zero, $\lambda_{2,a}$ may reduce to the mean free path, λ, in a three-dimensional ideal gas. Here we assume for $\lambda_{2,a}$

$$\lambda_{2,a}^{-1} = \lambda_{2,i}^{-1} + \bar{\xi} = 2D_0\sigma + \bar{\xi}$$

where $\bar{\xi}$ is an additional parameter which may be expressed approximately by $\bar{\xi} = a + bP$ for $P \leqq 10$ cmHg (a and b are constants independent of P) and $\bar{\xi}$ = constant ($= a + 10b$) for $P > 10$ cmHg. We have taken, for convenience, 10 cmHg as the transition point of $\bar{\xi}$ with no experimental evidence.

Since the diffusion coefficient of absorbed molecules, D_s, is given by one half of the product of the mean free path $\lambda_{2,a}$ and the mean velocity m_v, we obtain

$$D_s = (1/2)[1/(2D_0\sigma + \bar{\xi})](\pi kT/2m)^{1/2} \quad (14)$$

For a two-dimensional ideal gas ($\bar{\xi} = 0$), D_s approaches infinity as σ reduces to zero. In contrast to this, D_s for the absorbed molecuels varies from $(1/2\bar{\xi})(\pi kT/2m)^{1/2}$ at $\sigma = 0$ to $(1/4D_0\sigma)(\pi kT/2m)^{1/2}$ at $\sigma \gg \bar{\xi}/2D_0$.

Substituting σ in eq 12 into eq 11 and integrating across the membrane when $P = P_1$ at $x = 0$ and $P = P_2$ at $x = d$, we obtain

$$\begin{aligned}\dot{n}d = {} & (\pi r/2D_0)(\pi kT/2m)^{1/2} \\ & \times \ln \{\{v_{as}(P_1/P_0)/[(1-P_1/P_0) \\ & \times (1-P_1/P_0+\gamma P_1/P_0)] \\ & + \bar{\xi}/2D_0N_A\}/\{v_{as}(P_2/P_0)/[(1-P_2/P_0) \\ & \times (1-P_2/P_0+\gamma P_2/P_0)] + \bar{\xi}/2D_0N_A\}\} \\ & + (8/3)[(2-f_0)/f_0][\pi r^3/(2\pi mkT)^{1/2}] \\ & \times (P_2-P_1)\{1-[a(P_1)+a(P_2)]/2r\}^3 \end{aligned} \quad (15)$$

with

$$a(P_1)=D_0\gamma(P_1/P_0)/(1-P_1/P_0)\times(1-P_1/P_0+\gamma P_1/P_0)$$
$$a(P_2)=D_0\gamma(P_2/P_0)/(1-P_2/P_0)\times(1-P_2/P_0+\gamma P_2/P_0) \quad (16)$$

By comparing eq 15 with eq 7, we obtain

$$\boldsymbol{P}_c'(P_1, P_2)=\boldsymbol{P}_{s1}'+\{1-[a(p_1)+a(p_2)]/2r\}^3\boldsymbol{P}_f' \quad (17)$$

with

$$\boldsymbol{P}_{s1}'=[r(\pi RT)^{3/2}/z(P_2-P_1)2D_0N_A(2M)^{1/2}RT]\times\ln\{\{v_{as}\gamma(P_1/P_0)/[(1-P_1/P_0)\times(1-P_1/P_0+\gamma P_1/P_0)]+\bar{\xi}/2D_0N_A\}/\{v_{as}\gamma(P_2/P_0)/[(1-P_2/P_0)\times(1-P_2/P_0+\gamma P_2/P_0)]+\bar{\xi}/2D_0N_A\}\} \quad (18)$$

Gas Permeability Coefficient for a Porous Polymeric Membrane Having Straight-Through Cylindrical Pores

The number of pores having sizes between r and $r+dr$ per unit membrane area is defined by $N(r)dr$. Then $N(r)$ represents the pore radius distribution function.[9] If we find $N(r)$ for a given membrane, the pore number density N (number/cm^2), the i-th average pore radius $\bar{r}_i$, and the i-th moment of pore radius, X_i, can be calculated from

$$N=\int_{r_{min}}^{r_{max}}N(r)dr \quad (19)$$

$$\bar{r}_i=X_i/X_{i-1} \qquad i=1,2,3,\cdots \quad (20)$$

$$X_i=\int_{r_{min}}^{r_{max}}r^iN(r)dr=\bar{r}_i\bar{r}_{i-1}\cdots\bar{r}_1N \quad i=1,2,3,\cdots \quad (21)$$

where r_{min} and r_{max} are the minimum and maximum pore radii, respectively.

The overall gas permeability coefficient $\boldsymbol{P}(P_1, P_2)$ for a membrane in units of cm^3 (STP)/cm·s·cmHg, hereafter designated as PU, is expressed in terms of $\boldsymbol{P}_c(P_1, P_2)'$ as

$$\boldsymbol{P}(P_1, P_2)=\int_{r_{min}}^{r_{max}}\boldsymbol{P}_c(P_1, P_2)'N(r)dr(RT_s/P_s) \quad (22)$$

Here, RT_s/P_s is the coefficient for converting mol/cm·cmHg·s to PU, with T_s the standard temperature of 273.15 K and P_s the standard pressure of 76 cmHg.

Substitution of eq 8, 9, and 10 into eq 22 yields

$$\boldsymbol{P}(P_1, P_2)=\{X_1(\pi RT)^{3/2}(\ln P_1/P_2)/\times[z(P_1-P_2)2D_0N_A(2M)^{1/2}]+[(2-f_0)/f_0](4X_3/3)\times(2\pi RT/M)^{1/2}\}(T_s/P_s\cdot T) \quad (23)$$

Application of the definition of $\boldsymbol{P}(P_1, P_1)$ (*i.e.*, $\boldsymbol{P}(P_1, P_1)=\lim_{P_2\to P_1}\boldsymbol{P}(P_1, P_2)$) to eq 23 yields

$$\boldsymbol{P}(P_1, P_1)=\{X_1(\pi RT)^{3/2}/zP_1 2D_0N_A(2M)^{1/2}+[(2-f_0)/f_0](4X_3/3)\times(2\pi RT/M)^{1/2}\}(T_s/P_sT) \quad (24)$$

Following the same precedure used in deriving eq 23 and 24, we obtain from eq 17

$$\boldsymbol{P}(P_1, P_2)=\{\{X_1(\pi RT)^{3/2}/\times[z(P_1-P_2)2D_0N_A(2M)^{1/2}]\}\times\ln[v_{as}\gamma(P_1/P_0)/(1-P_1/P_0)\times(1-P_1/P_0+\gamma P_1/P_0)+\bar{\xi}/2D_0N_A]-\ln[v_{as}\gamma(P_2/P_0)/(1-P_2/P_0)\times(1-P_2/P_0+\gamma P_2/P_0)+\bar{\xi}/2D_0N_A]+[(2-f_0)/f_0](4/3)\{X_3-3[a(p_1)+a(p_2)]X_2/2+3[a(p_1)+a(p_2)]^2X_1/4-[a(p_1)+a(p_2)]^3N/8\}\times(2\pi RT/M)^{1/2}\}T_s/(P_sT) \quad (25)$$

and also,

$$\boldsymbol{P}(P_1, P_1)=\{\{X_1(\pi RT)^{3/2}/\times[z2D_0N_A(2M)^{1/2}]\}v_{as}(\gamma/P_0)[P_0{}^2+(\gamma-1)P_1{}^2]/\{v_{as}\gamma(P_1/P_0)/\times(1-P_1/P_0)[1-P_1/P_0+\gamma(P_1/P_0)]+\bar{\xi}/2D_0N_A\}(1-P_1/P_0)^2[1-P_1/P_0+\gamma(P_1/P_0)]^2+[(2-f_0)/f_0](4/3)\times[X_3-3a(p_1)X_2+3a(p_1)^2X_1-a(p_1)^3N](2\pi RT/M)^{1/2}\}(T_s/P_sT) \quad (26)$$

According to eq 26, the contribution of the S flow to the over-all gas flow may vary with the gas species

through the terms containing γ and P_0 and D_0. Thus, this contribution increases when the saturated vapour pressure P_0 decreases and/or when γ becomes large. Equations 25 and 26 are more general than eq 23 and 24.

The apparent activation energy E_p for gas permeation is defined by

$$E_p = -R[\mathrm{d} \ln \boldsymbol{P}(P_1, P_1)/\mathrm{d}(1/T)] \qquad (27)$$

The E_p value for free molecular flow is known theoretically to be about -0.3 kcal mol^{-1} at 300 K. Accordingly, the deviation of observed E_p from -0.3 kcal mol^{-1} may be taken as due to surface diffusion flow. The E_p value for this flow is evaluated from eq 9 or eq 18 to be about -0.3 kcal mol^{-1} or $[-0.3-(E_1-E_2)]$ kcal mol^{-1}, respectively. Since E_1 may be expressed as a function of interaction energy between gas molecule and polymer constituting the membrane and E_2 as a function of interaction energy between gas molecules, it is possible to estimate the interaction between gas molecule and membrane material from experimental E_p.

EXPERIMENTAL

Membrane Preparation

Commercially available polycarbonate membranes "nuclepore" (General Electric) designated Nu0.08, Nu0.05, Nu0.03, Nu0.015, and a non-alkali treated polycarbonate membrane designated Nu0.00 were used. In oreder to remove paraffin from the "nuclepore" membrane surface, the membranes as received were washed at 20°C with deethylether and dried *in vacuo*. The figures appearing with Nu indicate the nominal mean pore sizes in μm. These membranes have straight-through cylindrical pores and are quite suitable for quantitative gas permeation study. A homogeneous polycarbonate membrane Nus was cast from a chloroform solution. Note that Nu0.00 and Nus are not porous membranes.

A cellulose acetate membrane (SF0.54) was prepared by the micro-phase separation method[10] using a cellulose acetate sample (combined acetic acid content, 54.1 wt%; viscosity-average molecular weight, 1.05×10^5) in a mixture of $CaCl_2\cdot2H_2O$, acetone, methanol, and cyclohexanol. SF0.54 is a membrane containing spherical pores.[11]

Permeating Gases

Helium and argon were chosen as monoatomic gas, hydrogen, nitrogen, oxygen and carbon monooxide as diatomic gas, carbon dioxide as triatomic gas, and C_2H_2, C_2H_4, C_3H_6, C_3H_8, and C_4H_6 as organic gas. The purity of these gases was checked and confirmed to be more than 99.9 wt%.

Measurement

The porosity Pr of each membrane was determined by the apparent density method.[9] $N(r)$ of Nu0.08, Nu0.05, Nu0.03, and Nu0.015 were evaluated by scanning electron microscopy.[9] Since the experimental $N(r)$ values obtained in the region of small r were less reliable, the measured $N(r)$ curve was corrected by changing the absolute values of r determined by electronmicroscopy in such a way that $(\bar{r}_3\cdot\bar{r}_4)^{1/2}$ was equal the value determined by the water filtration rate method.[9] The correction factor was less than 0.1 for any case. The maximum pore radius r_{max} was determined by the bubble-point method.[9]

Gas permeability coefficients $\boldsymbol{P}(P_1, P_2)$ were measured using the same procedure as described in previous papers.[1-4] Most of the measurements were carried out at 25°C. The apparent activation energy E_p was obtained from the temperature dependence of $\boldsymbol{P}(P_1, P_2)$ according to eq 27.

RESULTS AND DISCUSSION

Membrane Characterization

Table I summarizes the values of N, $\bar{r}_i$ $(i=1-4)$, r_{max}, Pr, and X_i $(i=1-4)$ for the "nuclepore" membranes used.

Figure 2 illustrates $N(r)$ for these membranes. The porosity Pr and the mean pore radius $(\bar{r}_3\cdot\bar{r}_4)^{1/2}$ obtained by the water filtration rate method for Nu0.00, Nus and SF0.54 are given in Table II.

Permeation of Inorganic Gas

Gas permeation mechanisms for porous membranes may be classified into the following six cases, A through F, in terms of the mean free path at the inlet of the membrane pore λ_1, that at the outlet λ_2, r_{min}, and r_{max}[3,4]:

Case A, $2r_{min}>\lambda_2$; Case B, $\lambda_1<2r_{min}\leqq\lambda_2<2r_{max}$; Case C, $2r_{min}\leqq\lambda_1$ and $2r_{max}>\lambda_2$; Case D, $\lambda_1<2r_{min}\leqq2r_{max}\leqq\lambda_2$; Case E, $2r_{min}\leqq\lambda_1<2r_{max}\leqq\lambda_2$; Case F, $2r_{max}\leqq\lambda_1$.

Table I. Characterization of pores in polycarbonate membranes

Membrane code	Nu0.8	Nu0.6	Nu0.2	Nu0.1
N (number/cm^2)	5.42×10^{7}	9.1×10^{7}	2.1×10^{8}	8.0×10^{8}
$\bar{r}_i$ $i=1$ (μm)	0.356	0.235	0.118	0.0629
$i=2$ (μm)	0.456	0.252	0.132	0.0715
$i=3$ (μm)	0.501	0.268	0.156	0.0840
$i=4$ (μm)	0.567	0.325	0.183	0.0984
r_{max} (μm)	0.580	0.34	0.19	0.11
r_{min} (μm)	0.10	0.10	0.045	0.028
Pr (—)	0.22	0.14	0.13	0.10
X_i $i=1$ (cm^{-1})	1.93×10^{3}	2.15×10^{3}	2.48×10^{3}	5.05×10^{3}
$i=2$ (—)	6.87×10^{-2}	5.41×10^{-2}	3.26×10^{-2}	3.61×10^{-2}
$i=3$ (cm)	3.45×10^{-6}	1.45×10^{-6}	5.09×10^{-7}	3.03×10^{-7}
$i=4$ (cm^2)	1.95×10^{-10}	4.71×10^{-11}	9.31×10^{-12}	2.99×10^{-12}

Membrane code	Nu0.08	Nu0.05	Nu0.03	Nu0.015
N (number/cm^2)	6.83×10^{8}	3.91×10^{8}	1.62×10^{7}	1.03×10^{9}
$\bar{r}$ $i=1$ (μm)	5.60×10^{-2}	4.70×10^{-2}	1.74×10^{-2}	2.21×10^{-2}
$i=2$ (μm)	5.99×10^{-2}	4.71×10^{-2}	1.80×10^{-2}	2.22×10^{-2}
$i=3$ (μm)	6.56×10^{-2}	4.75×10^{-2}	1.86×10^{-2}	2.27×10^{-2}
$i=4$ (μm)	7.13×10^{-2}	4.96×10^{-2}	1.92×10^{-2}	2.32×10^{-2}
r_{max} (μm)	1.82×10^{-1}	6.6×10^{-2}	3.4×10^{-2}	3.2×10^{-2}
r_{min} (μm)	2.5×10^{-2}	1.8×10^{-2}	0.7×10^{-2}	1.3×10^{-2}
Pr (—)	0.072	0.026	0.020	—
X_i $i=1$ (cm^{-1})	3.83×10^{3}	1.80×10^{3}	2.82×10	2.35×10^{3}
$i=2$ (—)	2.29×10^{-2}	8.45×10^{-3}	5.09×10^{-5}	5.20×10^{-3}
$i=3$ (cm)	1.50×10^{-7}	4.01×10^{-8}	9.46×10^{-11}	1.18×10^{-8}
$i=4$ (cm^2)	1.07×10^{-12}	1.99×10^{-13}	1.81×10^{-16}	2.74×10^{-14}

Figure 3 shows the pressure dependence of $\boldsymbol{P}(P_1, P_2)$ for some typical inorganic gases in Nu0.03, Nu0.015, Nu0.00, and Nus. Most of the data for Nu0.03 were taken from our previous papers,[3,4] in which the theoretical value of $\boldsymbol{P}(P_1, P_1)$ in case F was approximated by the second term of eq 24. This approximation cannot be applied to the case where the permeating gas is organic and the mean pore size is less than 18 nm. The broken lines in Figure 3 indicate $\boldsymbol{P}(P_1, P_1)$ and the dotted lines $\boldsymbol{P}(P_1, 0)$ where both obtained by extrapolating the experimental $\boldsymbol{P}(P_1, P_2)$ values.

We can evaluate $\boldsymbol{P}(0, 0)$ by first extrapolating experimental $\boldsymbol{P}(P_1, P_2)$ to $P_1=P_2$ and then the result to $P_1=0$. The $\boldsymbol{P}(0, 0)$ values thus obtained are plotted against $X_3M^{-1/2}$ in Figure 4, where previous data[3] are also shown. The straight line represents $\boldsymbol{P}(P_1, P_1)$ for the F flow (denoted by $\boldsymbol{P}_f$) calculated from eq 26 with $f_0=1.0$, and $\gamma=0$ at 293.15 K, where $\boldsymbol{P}_f$ is given by

$$\boldsymbol{P}_f=(4/3)X_3(2\pi RT/M)^{1/2}(T_s/P_sT) \qquad (28)$$

The data points fall well on the theoretical line for $\boldsymbol{P}_f$, indicating that when $\gamma=0$, $\boldsymbol{P}(P_1, P_1)$ of in-

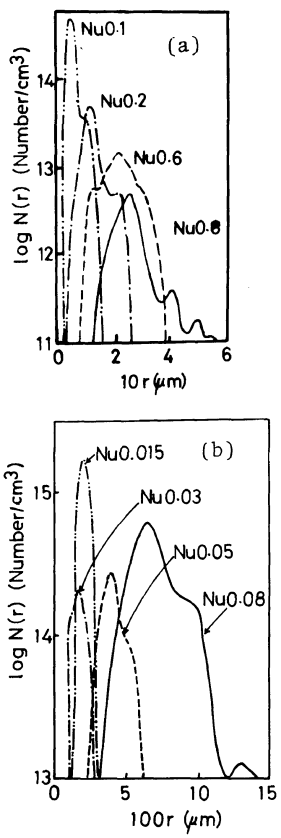

Figure 2. Distribution functions of pore radius for various polycarbonate membranes determined by electron scanning microscopy.

Table II. Porosity Pr and mean pore radii $(\bar{r}_3 \cdot \bar{r}_4)^{1/2}$ for membranes Nu0.00, Nus, and SF0.54

Membrane code	Nu0.00	Nus	SF0.54
Pr (%)	7.1×10^{-4} [a]	10^{-6}	54.0
$(\bar{r}_3 \cdot \bar{r}_4)^{1/2}$ (nm)	1.5	1.2	50

[a] Calculated from experimental $(\bar{r}_3 \cdot \bar{r}_4)^{1/2}$ using $Pr = \pi(\bar{r}_3 \cdot \bar{r}_4)N$, and with N taken to be 10^8 (No./cm^2).

organic gases for polycarbonate membranes having $\bar{r}_3$ larger than 18.0 nm can be attributed to free molecular flow alone.

The plots of $\boldsymbol{P}(0, 0)$ for Nu0.00 and Nus against $M^{-1/2}$ are shown in Figure 5. The filled circles are the values for Nu0.00 and the unfilled circles for Nus. The theoretical values of $\boldsymbol{P}_f$ are represented by the dot-dash line for Nu0.00 and the dashed line for Nus. The calculation of $\boldsymbol{P}_f$ was made by taking X_3 to be 1.31×10^{-13} cm for Nu0.00 and 9.63×10^{-14} cm for Nus. These values of X_3 were obtained by putting the experimental value of $\boldsymbol{P}(P_1, P_1)$ for He into eq 28 on the assumption that the He gas passes through the membrane only by free molecular flow. It should be noted that the $\boldsymbol{P}(0, 0)$ values for CO_2 in both Nu0.00 and Nus membranes are larger than those for N_2, in agreement with the usual observations of gas permeation through dense polymer membranes. The $\bar{r}_3$ value can also be evaluated from $\boldsymbol{P}(0, 0)$ by the method proposed before,[12] and gives about 1.2 nm for Nu0.00. This $\bar{r}_3$, through somewhat smaller than the one gives in Table II, is used below for the mean pore radius of Nu0.00.

Permeation of Organic Gas

Figure 6 shows the dependence of $\boldsymbol{P}(P_1, P_2)$ on the average pressure $\bar{P}(=(P_1+P_2)/2)$ for various organic gases in Nu0.08, Nu0.03, Nu0.015, and Nu0.00. In contrast to those of inorganic gases, $\boldsymbol{P}(0, 0)$ of organic gases do not agree with the values calculated from eq 26 with $\gamma = 0$.

Figure 7 illustrates the $\boldsymbol{P}(0, 0)$ values for C_4H_6 (filled circle) and C_3H_8 (unfilled circle) in Nu0.08, Nu0.03, Nu0.015, and Nu0.00 plotted against $X_3M^{-1/2}$. The X_3 for Nu0.00 was evaluated from the observed $\boldsymbol{P}(0, 0)$ for He. The full line represents theoretical values of $\boldsymbol{P}_f$ (eq 28), and the hatched area indicates the range of experimental $\boldsymbol{P}(0, 0)$ values ascribable to the dissolution/diffusional flow (the D flow). It can be seen that positive deviations of experimental $\boldsymbol{P}(0, 0)$ from the theoretical line reach a maximum at an $X_3M^{-1/2}$ close to 10^{-11} (cm·mol$^{1/2}$/g$^{1/2}$). The extent of this deviation varies with the kind of gas species. Hereafter, the flow relating to this deviation is called the SD flow, and its gas permeation coefficient is denoted by $\boldsymbol{P}_{sd}(P_1, P_1)$.

It should be noted that the overall gas permeation coefficient $\boldsymbol{P}(P_1, P_1)$ has the same order of magnitude as that for the F flow even if the SD flow cannot be neglected. If $\boldsymbol{P}_{sd}(P_1, P_1)$ has the same X_i and the same gas species dependence as $\boldsymbol{P}_s$ and, furthermore, if $\boldsymbol{P}_{sd}(P_1, P_1)$ agrees quantitatively with $\boldsymbol{P}_s(P_1, P_1)$ calculated from eq 26, the SD flow may be regarded as being similar to the S flow that occurs with $\gamma \neq 0$.

Analysis of the permeability coefficient data obtained by Adzumi[13] for glass capillary shows no

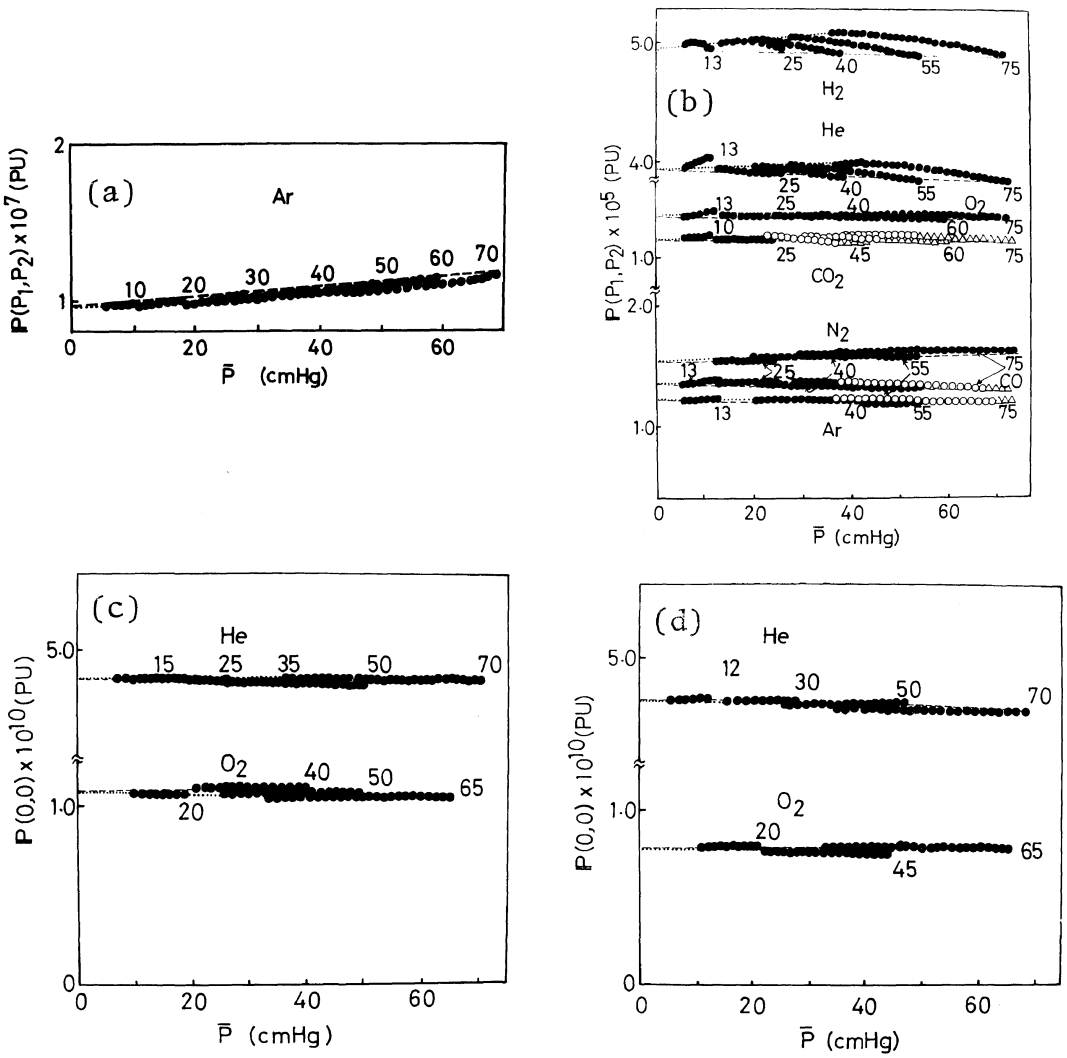

Figure 3. $\bar{P}$ dependence of $P(P_1, P_2)$ for inorganic gases in polycarbonate membranes Nu0.03, Nu0.015, Nu0.00 and Nus: broken lines, $P(P_1, P_1)$; dotted lines, $P(P_1, 0)$. Figures on the curves denote P_1 in cmHg. All marks are experimental data points: ●, case F; ○, case E; ▲, case D; △, case C. (a), Nu 0.03; (b), Nu0.015; (c) Nu0.00; (d), Nus.

difference between organic and inorganic gases. The discrepancy between Adzumi's and our observations may be due to the great difference in the type of material of the pore wall, pore size, and surface area of the pore wall.

The coefficient $P_{sd}(P_1, P_1)$ is expressed, according to definition, by

$$P_{sd}(P_1, P_1) = P(P_1, P_1) - [(2-f_0)/f_0] \times (4/3)X_3(2\pi RT/M)^{1/2}(T_s/P_sT) \quad (29)$$

The second term agrees with P_f in eq 28 when f_0 equals one. $P_{sd}(P_1, P_1)$ can be evaluated by putting the experimental values of $P(P_1, P_1)$, X_3, T and M and also the semi-empirical value of f_0 given in the literature[1-3] into eq 29.

The value of $P(P_1, P_1)$ extrapolated to $P_1 = 0$ is nearly the same as that at $P_1 = 5$ cmHg, which is the experimentally measurable minimum pressure with 10% accuracy, so that we regard $P(5, 5)$ as equal to $P(0, 0)$.

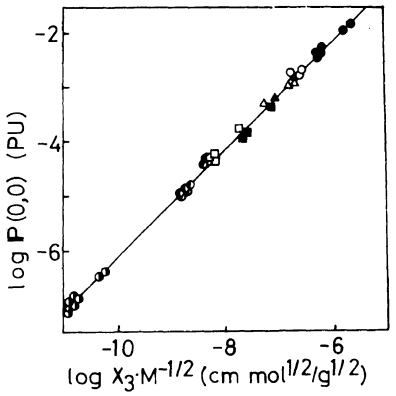

Figure 4. Log-log plot of $P(0,0)$ against $X_3M^{-1/2}$: ●, Nu0.8; ○, Nu0.6; ▲, Nu0.2; △, Nu0.1; ■, Nu0.08; □, Nu0.05; ◑, Nu0.03; ◐, Nu0.015.

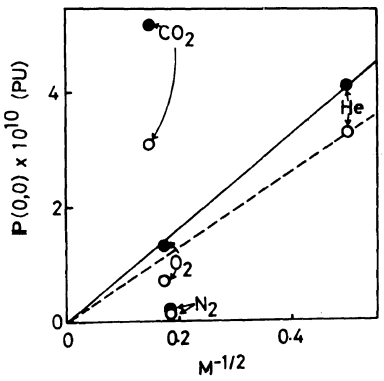

Figure 5. $M^{-1/2}$ dependence of $P(0,0)$ for Nu0.00 and Nus: —, theoretical P_f (free molecular flow) for Nu0.00; – – –, theoretical P_f for Nus; ●, experimental $P(0,0)$ for Nu0.00; ○, experimental $P(0,0)$ for Nus.

Figure 8 shows the values of $P_{sd}(0,0)$ plotted against $(M^{1/2}P_0)^{-1}$ for Nu0.03. $P_{sd}(0,0)$ increases with an increase in $(M^{1/2}P_0)^{-1}$, as in the case of the F flow given by eq 28 for the gases having the same P_0 value.

The dependence of $P_{sd}(0,0)$ for C_4H_6 on X_i ($i=1$, 2, 3) is shown in Figure 9. The linear dependence of $P_{sd}(0,0)$ on X_1 appears to be most likely, and is represented by

$$P_{sd}(0,0)=6.6\times10^{-10}X_1 \quad [(\text{PU}) \text{ for } C_4H_6/\text{polycarbonate}] \qquad (30)$$

This linear X_1 dependence of $P_{sd}(0,0)$ is the same as expected from eq 32 for the S flow.

When the ratio $P_{sd}(0,0)/P(0,0)$ is plotted against $\bar{r}_3$ (see Figure 10), we find that only in a certain limited range of $\bar{r}_3$ can the SD flow be observed clearly. As evident from Figure 10, $P_{sd}(0,0)$ makes a significant contribution to the overall gas permeability coefficient only at pore radii ranging from 15 nm to 1.2 nm for both C_4H_6 and C_3H_8.

Figure 11 shows the plots of $P(0,0)$ against $M^{-1/2}$ for various organic gases in the polycarbonate membrane Nu0.015. The open marks indicate $P(0,0)$ obtained by the double extrapolation mentioned above. The experimental values shown were obtained with the membrane having a virgin surface, *i.e.*, the membrane cleaned with the helium gas for 4 h. The closed marks are the values taken after a given organic gas permeated a membrane for 2 h or more, and the full line represents the theoretical values of P_f calculated from eq 28. As a result of helium gas permeation prior to each permeation experiment $P(0,0)$ increased greatly, and when the molecular weight of the gas was larger than 43, $P(0,0)$ exceeded even the theoretical P_f. With an increase in molecular weight of an organic gas, the difference between $P(0,0)$ for the membrane with a virgin surface and P_f increased. Even if the membrane was placed in an organic gas for 69 h or longer at 25°C, the membrane neither deformed nor swelled (see Table III). It can be seen from Figure 11 that one factor leading to a negative value of $P_{sd}(0,0)$, as illustrated for C_3H_8 in Figure 10, is the narrowing of pores due to the sorption of molecules on the pore wall. The adsorbed molecules are purged by permeation of the helium gas, causing $P_{sd}(0,0)$ to take on a positive value.

Gas Permeability Coefficient for the Surface Diffusion Flow

By putting eq 24 or eq 26 into eq 29, we obtain eq 31 or eq 32, respectively.

$$P^h_{sd}(P_1,P_1)=[X_1(\pi RT)^{3/2}/zP_1 2D_0N_A(2M)^{1/2}](T_s/P_sT) \qquad (31)$$

$$P^i_{sd}(P_1,P_1)=[X_1(\pi RT)^{3/2}/z2D_0Na(2M)^{1/2}]\times(T_s/P_sT)v_{as}\gamma(1/P_0)^3[P_0{}^2+(\gamma-1)P_1{}^2]/\{\{v_{as}\gamma(P_1/P_0)/(1-P_1/P_0)[1-P_1/P_0+\gamma(P_1/P_0)]+\bar{\xi}/2D_0N_A\}(1-P_1/P_0)^2[1-P_1/P_0$$

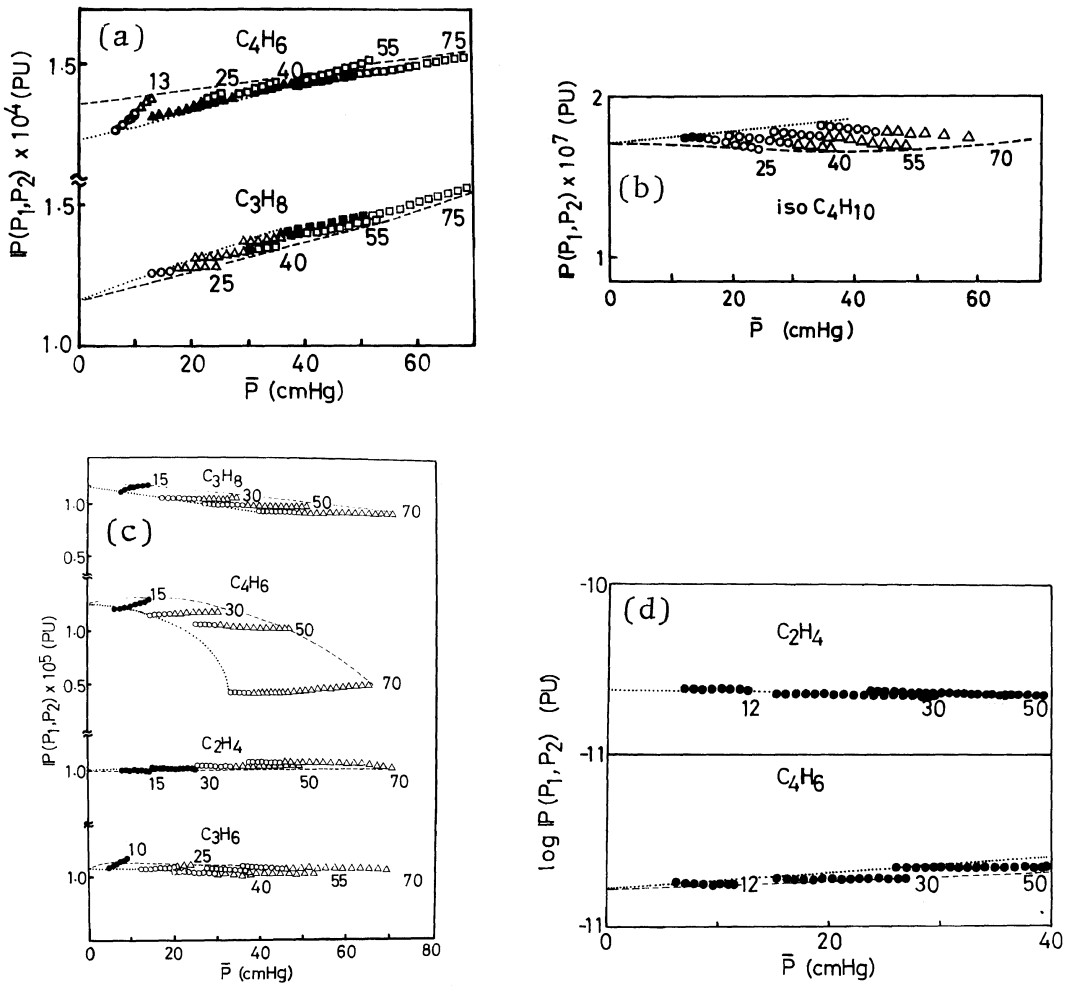

Figure 6. $\bar{P}$ dependence of $\boldsymbol{P}(P_1, P_2)$ for organic gases in polycarbonate membranes: broken line, $\boldsymbol{P}(P_1, P_1)$; dotted line, $\boldsymbol{P}(P_1, 0)$. Figures on the curves denote P_1 in cmHg and the data point marks have the same meaning as in Figure 3. (a), Nu0.08; (b), Nu0.03; (c), Nu0.015; (d), Nu0.00.

$$+\gamma(P_1/P_0)]^2\}-[(2-f_0)/f_0]$$
$$\times(4/3)X_3[3a(p_1)/\bar{r}_3-3a(p_1)^2/$$
$$\times\bar{r}_3\cdot\bar{r}_2+a(p_1)^3/\bar{r}_1\cdot\bar{r}_2\cdot\bar{r}_3]$$
$$\times(2\pi RT/M)^{1/2}(T_s/P_sT) \qquad (32)$$

Here, the superscripts h and i indicate that $\boldsymbol{P}_{sd}$ has been derived from the equation of Hill (eq 5) and its improved equation (eq 11), respectively.

Experimentally, we found that:

(A) $\boldsymbol{P}_{sd}(0, 0)$ increased with an increase in $(M^{1/2}P_0)^{-1}$ (see Figure 8),

(B) $\boldsymbol{P}_{sd}(0, 0)$ for C_4H_6 showed a linear dependence on X_1 (see, Figure 9)

(C) $\boldsymbol{P}_{sd}(0, 0)/\boldsymbol{P}(0, 0)$ for $C_4H_6$and C_3H_8 reached maxima at pore radii between 15 and 1.2 nm (see Figure 10)

(D) During the organic gas permeation, $\boldsymbol{P}_{sd}(0, 0)$ for C_4H_6 and C_3H_8 decreased and eventually became negative. When the membrane surface was cleaned by helium gas, $\boldsymbol{P}_{sd}(0, 0)$ resumed a positive initial value after a long run (see Figure 11).

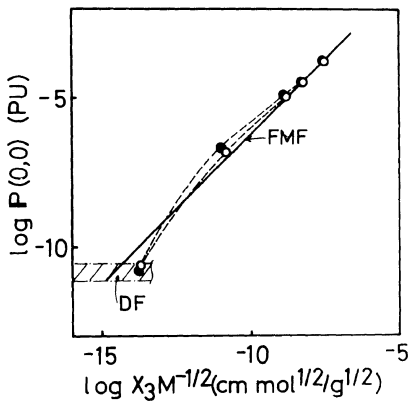

Figure 7. $X_3M^{-1/2}$ dependence of $P(0,0)$ for C_4H_6 and C_3H_8 in a polycarbonate membrane: ●, experimental $P(0,0)$ for C_4H_6; ○, experimental $P(0,0)$ for C_3H_8; straight line, theoretical $P(0,0)$ of free molecular flow. The hatched region indicates experimental values for gas permeation due to the dissolution/diffusional flow.

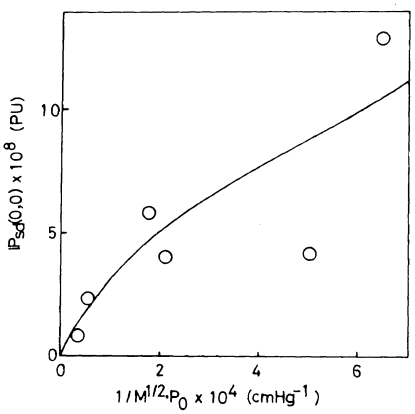

Figure 8. Plots of $P_{sd}(0,0)$ against $1/M^{1/2}P_0$ for Nu0.03.

Equation 31 fails to explain (A), (C), and (D). On the other hand, eq 32 can explain all these experimental findings quantitatively as described below:

When P_1 approaches zero, the theoretical $P_{sd}(0, 0)$ calculated by eq 32 is nearly proposional to $(M^{1/2}P_0)^{-1}$, as confirmed experimentally. The finding (B) can be well explained by eq 32. Since the contribution of the F flow increases more remarkably than the SD flow, the $\bar{r}_3$ dependence of $P(0, 0)$ is more significant than that of $P_{sd}(0, 0)$. Therefore, the ratio $P_{sd}(0, 0)/P(0, 0)$ decreases with an icnrease in $\bar{r}_3$. On the other hand, a decrease in $\bar{r}_3$ accompanying a decrease in X_1 makes $P_{sd}(0, 0)$ small and also makes the contribution of the D flow to the overall gas permeation large, but that of the F flow small. The decrease in $P_{sd}(0, 0)$ gives rise to a decrease in $P_{sd}(0, 0)/P(0, 0)$. Consequently,

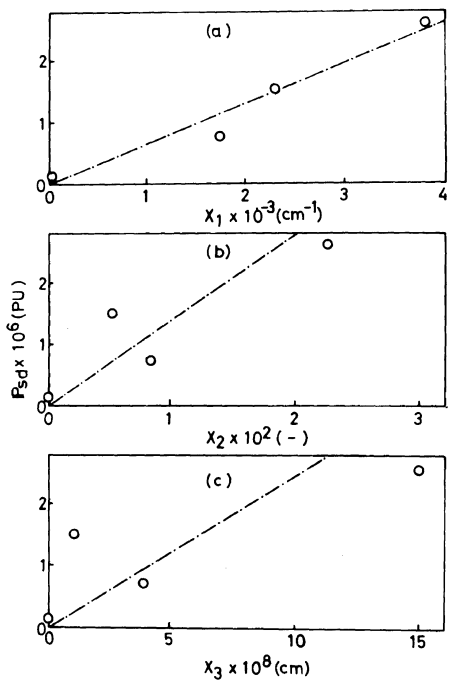

Figure 9. Plots of $P_{sd}(0, 0)$ against X_i ($i=1, 2, 3$): (a), $i=1$; (b), $i=2$; (c), $i=3$.

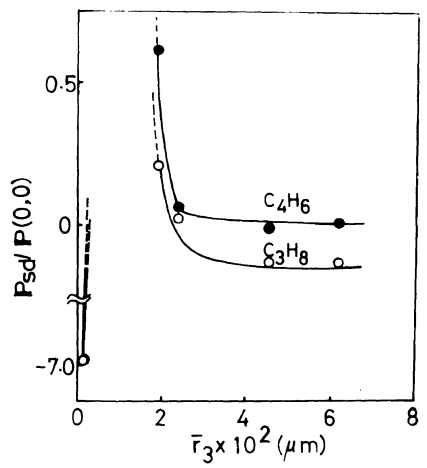

Figure 10. $\bar{r}_3$ dependence of $P_{sd}(0, 0)/P(0, 0)$ for C_3H_8 and C_4H_6 in a polycarbonate membrane: ○, C_3H_8; ●, C_4H_6.

Table III. Swelling deformation of polycarbonate membranes in C_4H_6 gas at 20°C and 1 atm.

Time	Nu0.6		Nu0.03		Nu0.015	
	Thickness	Diameter	Thickness	Diameter	Thickness	Diameter
min	μm	mm	μm	mm	μm	mm
0	10.5	4.70	5.5	4.70	5.7	4.70
180	10.5	4.70	5.5	4.70	5.7	4.70
4200	10.5	4.70	5.5	4.68	5.9	4.70

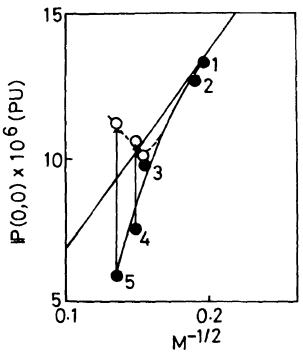

Figure 11. $M^{-1/2}$ dependence of $P(0,0)$ for organic gases in Nu0.015: 1, C_2H_2; 2, C_2H_4; 3, C_3H_6; 4, C_3H_8; 5, C_4H_6. Filled circle indicates the $P(0,0)$ value after 2 h permeation of a given organic gas, and unfilled circle the value after 4 h permeation of helium gas. Straight line indicates the theory of the F flow.

$P_{sd}(0,0)/P(0,0)$ has a maximum at a certain $\bar{r}_3$ as indicated in the finding (C). When gas molecules tend to be adsorbed on the membrane surface and the pore wall, the thickness of the absorbed gas layer, $a(p_1)$, increases with γ, yielding a negative value for $P_{sd}(0,0)$, as predicted from eq 32. This is the experimental finding (D).

We can thus definitely conclude that eq 32 is preferable to eq 31 for describing observed $P_{sd}(0,0)$ and that the improved theory including the contribution of surface diffusion (eq 32) explain reasonably the difference between the experimentally observed total gas coefficient $P(P_1, P_1)$ and theoretical P_f.

Numerical calcualtions for eq 26 and 32 were carried out with $M=40$, $D_0=5\times10^{-8}$ cm, $T=300$ K, and $v_{as}=8.49\times10^{-10}$ mol/cm^2. P_f was found to be 6.29×10^3 M$^{-1/2}X_3$ (PU) through the numerical calculation of eq 28. $\bar{\xi}$ was assumed to be $(P_1+10)/1.68\times10^{-4}$ by taking into consideration the boundary conditions such that when P_1 approaches 5 cmHg, $1/\bar{\xi}$ approaches λ $(=\eta(\pi RT)^{1/2}-(2M)^{1/2}zP_1)$ at $P_1=5$ cmHg. Here, η is the viscosity of the gas taken approximately to be 0.72×10^{-4} poise as a typical value for organic gases.

Figure 12 shows $P(P_1, P_1)$ thus calculated for the polycarbonate membrane Nu0.03. The theoretical $P(P_1, P_1)$ decreases with increasing P_1, regardless of P_0 if γ is larger than 1.0. In limited ranges of γ and P_0, such as $\gamma=0.01$ and $P_0=100$ cmHg, this $P(P_1, P_1)$ increases with an increase in P_1. The molecular weight of 40 used in this calculation is nearly equal to that of C_3H_6 ($M=42$) whose vapor pressure is 858.2 cmHg.[14] The calculated $P(P_1, P_1)$ for $\gamma=0.16$ and $P_0=1500$ cmHg in Figure 12(b) is quite consistent with the dashed line in Figure 6(b).

The gas permeation coefficient of the S flow for a membrane having a pore size distribution $N(r)$ is given by

$$P_s(P_1,P_1)=\int_{r_{min}}^{r_{max}} P_{s1}'N(r)dr(RT_s/P_s) \tag{33}$$

Substitution of eq 18 into eq 33 leads to

$$\begin{aligned}P_s(P_1,P_1)=&\{[X_1(\pi RT)^{3/2}]/\\&\times[z2D_0Na(2M)^{1/2}]\}(T_s/P_sT)v_{as}(\gamma/P_0)\\&\times(1/P_0)^2[P_0^2+(\gamma-1)P_1^2]/\\&\times\{(1-P_1/P_0)^2[1-P_1/P_0\\&+\gamma(P_1/P_0)]^2v_{as}\gamma(P_1/P_0)/(1-P_1/P_0)\\&\times[1-P_1/P_0+\gamma(P_1/P_0)]\\&+\bar{\xi}/2D_0N_A\}\end{aligned} \tag{34}$$

Hereafter, $P_s(P_1, P_2)$, $P_{sd}(P_1, P_2)$, and $P(P_1, P_2)$ are calculated using this improved equation for the S flow.

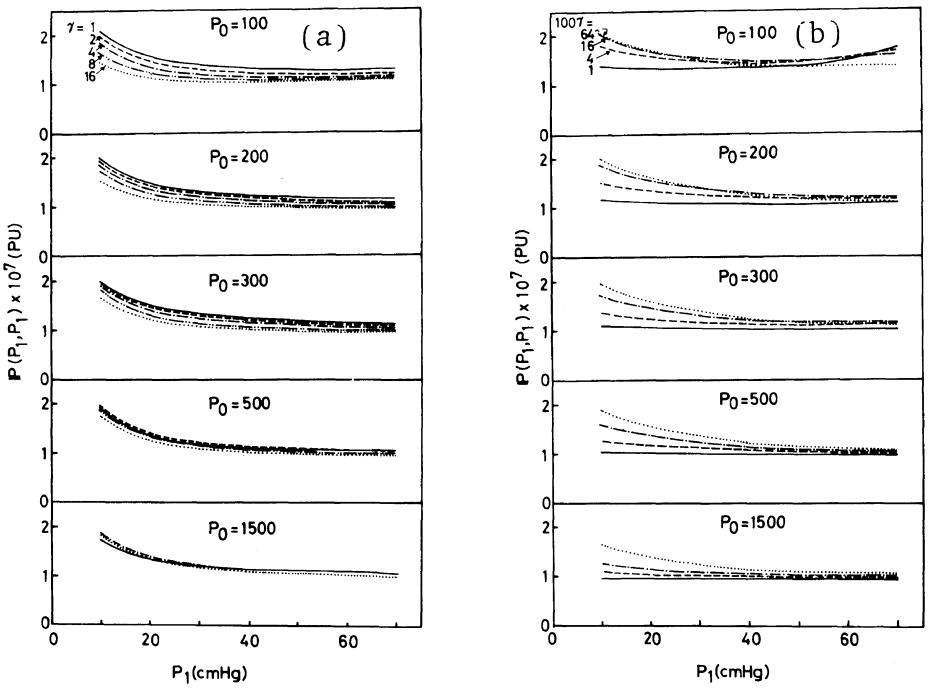

Figure 12. P_1 dependence of $P(P_1, P_1)$ for Nu0.03 calculated by use of eq 26: ——, $\gamma=1$; – – –, $\gamma=2$; – – –, $\gamma=4$; – – –, $\gamma=8$; ------, $\gamma=16$ in Figure 12(a). ——, $\gamma=0.01$; – – –, $\gamma=0.04$; – – –, $\gamma=0.16$; ------, $\gamma=0.64$ in Figure 12(b).

Values of $P_s(10, 10)$, $P_{sd}(10, 10)$, and $P_{sd}(10, 10)/P(10, 10)$ were calculated for $P_1=10$ cmHg. The results obtained are shown in Figure 13. The calculated $P_s(10, 10)$, $P_{sd}(10, 10)$, and $P_{sd}(10, 10)/P(10, 10)$ decrease with increasing P_0 in the range $\gamma \leqq 2$ and attain maxima at certain values of P_0 for $\gamma > 2$. $P_{sd}(10, 10)/P(10, 10)$ for $\gamma=0.16$ in Nu0.03 decreases from 0.54 at $P_0=100$ cmHg to 0.19 at $P_0=2500$ cmHg with an increase in P_0 and this range of $P_{sd}(10, 10)/P(10, 10)$ covers most of the previously observed values of $P_{sd}(0, 0)/P(0, 0)$ for Nu0.03.[3] For an inorganic gas which has a P_0 higher than 1500 cmHg and a small γ, $P_{sd}(10, 10)/P(10, 10)$ should approach zero. This expectation is confirmed by the experimental values reported previously.[1-3]

The gas permeation coefficient of the S flow given by eq 34 has a maximum at a certain value of γ. Figure 14 show the γ dependence of $P_s(10, 10)$ given by eq 34. The maximum of $P_s(10, 10)$ decreases with increasing P_0, giving a large γ for the maximum position. Thus, the maximum contribution of the S flow to gas permeation in a given membrane should occur at a specific combination of P_0 and γ. The parameter γ depends on the interaction between the gas molecules and the membrane material, while P_0 depends only on the gas species at a given temperature.

Both experiment and theory show that the gas permeation coefficient P_f, P_s, and P_d are proportional to X_3, X_1, and $(1-Pr)$, respectively. Here, the subscripts f, s, and d indicate the F, S, and D flows, respectively. The great difference in X_i dependence of $P(P_1, P_1)$ leads to the speculation that since a larger i and X_i gives rise to further increment of X_i with an increase in pore size, $P_s/P(P_1, P_1)$, which is proportional to $X_1/[X_3+(1-Pr)]$, may have a maximum at a certain value of pore size for membranes having similar pore size distributions. The S flow is expected to be observed only in the limited range of pore size. Figure 15 illustrates the $\bar{r}_3$ dependence of X_1/X_3 and $X_1/(1-Pr)$ for a series of polycarbonate membranes. X_1/X_3 represents the ratio of the gas permeation coefficients for S and F flow and $X_1/(1-Pr)$, the corresponding ratio for D and F flow. When $\bar{r}_3$ is large, the F flow dominates,

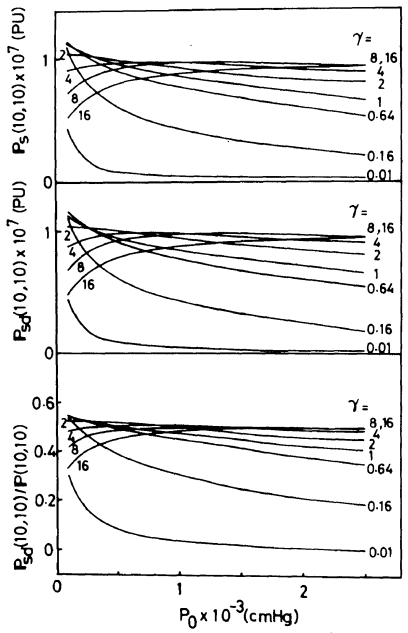

Figure 13. Theoretical gas permeation coefficient $P_s(10, 10)$ and $P_{sd}(10, 10)$, and the ratio of $P_{sd}(10, 10)$ to $P(10, 10)$ as a function of P_0 for Nu0.03: The figures denote γ values.

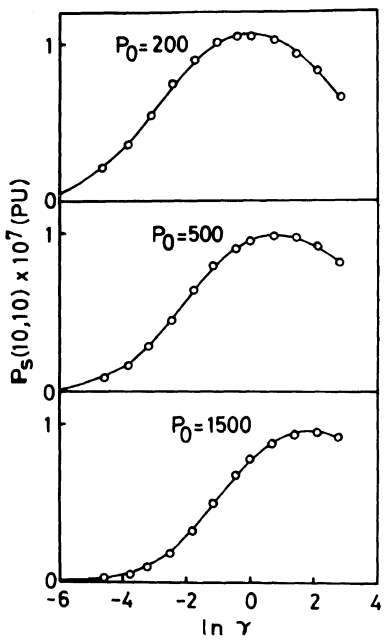

Figure 14. γ dependence of theoretical P_s for Nu0.03.

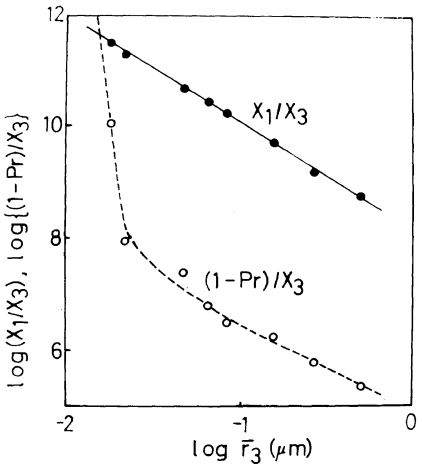

Figure 15. Plots of X_1/X_3 and $(1-Pr)/X_3$ against $\bar{r}_3$ for a polycarbonate membrane.

Table IV. Apparent activation energy E_p for gas permeation at 30°C

Gas species	E_p/kcal mol^{-1}		
	SF0.54	Nu0.00	Nus
H_e	−0.26	2.30	4.09
N_2	−0.63	3.85	5.96
O_2	−0.46	1.80	4.24
CO	−0.67	2.94	—
CO_2	—	2.02	3.25
C_2H_4	−0.87	3.64	—
C_4H_6	—	0.51	—

while when $\bar{r}_3$ is small, the D flow dominates, as illustrated in Figure 15.

The S flow may be observed even in gas permeation through a cellulose acetate membrane whose pore size distribution is broad and whose pore shape is rather irregular, compared with those of the polycarbonate membranes studied here. Figure 16 shows the reciprocal temperature dependence of the experimental $P(0, 0)$ for various gases in a cellulose acetate membrane SF0.54. Table IV summarizes the values of E_p calculated by eq 27. It can be seen from Figure 16 that the E_p values for both Nu0.00 and Nus are associated with the activation energy for the D flow. The E_p value of C_2H_4 for SF0.54 is about −0.87 kcal mol^{-1}, while those of inorganic gases are in the range −0.26 to −0.67 kcal mol^{-1}, as expected theoretically for the

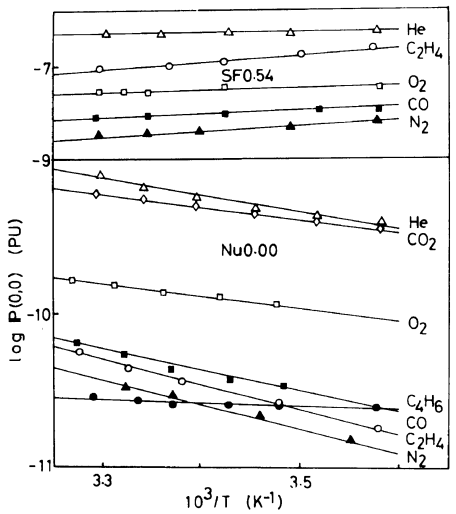

Figure 16. Reciprocal temperature dependence of permeability coefficient $P(0, 0)$ of various gases for cellulose acetate membrane SF0.54 and polycarbonate membrane Nu0.00: ○, C_2H_4; ●, C_4H_6; △, H_e; ▲, N_2; □, O_2; ■, CO.

F flow. The E_p value for the S flow depends not only on the temperature dependence of γ, but also on P_0 as can be found from eq 34. Accordingly, it must vary from values less than -0.4 kcal mol^{-1} corresponding to the F flow to values above that corresponding to the D flow.

CONCLUSIONS

When the pore size of a porous polymeric membrane decreased below a certain value, which depends on both the membrane material and the permeating gas, the gas permeability coefficient exceeds the value for free molecular flow, especially in the case of organic gases. This phenomenon can be attributed to the surface diffusion flow. The permeability coefficient for this flow has been theoretically evaluated in the present paper. The surface diffusion flow may be observed in a limited range of pore size even for an inorganic gas. The question as to whether a mixed gas can be separated into its individual components by utilizing this flow remains for future study.

REFERENCES

1. T. Nohmi, S. Manabe, K. Kamide, and T. Kawai, *Kobunshi Ronbunshu*, **34**, 729 (1977).
2. T. Nohmi, S. Manabe, K. Kamide, and T. Kawai, *Kobunshi Ronbunshu*, **34**, 737 (1977).
3. T. Nohmi, H. Makino, S. Manabe, K. Kamide, and T. Kawai, *Kobunshi Ronbunshu*, **35**, 253 (1978).
4. K. Kamide, S. Manabe, T. Nohmi, H. Makino, H. Narita, and T. Kawai, "Polymer Separation Media," A. T. Cooper, Ed., Plenum Press, New York, 1982, p 35.
5. G. W. Sears, *J. Chem. Phys.*, **22**, 1252 (1954).
6. T. L. Hill, *J. Chem. Phys.*, **25**, 730 (1956).
7. For example E. A. Moelwyn-Hughes, "Physical Chemistry," Pergamon Press, Oxford, 1961, p 966.
8. For example S. Glasstone, "The Elements of Physical Chemistry," Maruzen Company, Ltd., Tokyo, 1954, p 91.
9. K. Kamide and S. Manabe, "Ultrafiltration Membranes and Applications," A. R. Cooper, Ed., Plenum Press, New York, 1980, p 173.
10. K. Kamide, S. Manabe, T. Matsui, T. Sakamoto, and S. Kajita, *Kobunshi Ronbunshu*, **34**, 205 (1977).
11. S. Manabe, K. Kamide, T. Nohmi, and T. Kawai, *Kobunshi Ronbunshu*, **37**, 405 (1980).
12. T. Nohmi, S. Manabe, K. Kamide, and T. Kawai, *Kobunshi Ronbunshu*, **35**, 509 (1978).
13. H. Adzumi, *Bull. Chem. Soc. Jpn.*, **12**, 199 (1937).
14. The American Chemical Society, Ed., "Physical Preperties of Chemical Compounds II," (Advances in Chemical Series, Vol. 22), The American Chemical Society, Washington, D. C., 1959.